

Electronic Supplementary Information (ESI)

Cucurbit[6]uril-based carbon dots for recognizing *L*-Tryptophan and Capecitabine

Ming Liu,^a Ran Cen,^a Ji-Hong Lu,^a Tie-Hong Meng,^{b*} Chun-Rong Li,^b Carl Redshaw,^{c*} Timothy J. Prior,^c Zhu Tao,^a Xin Xiao^{a*}

^a Key Laboratory of Macrocyclic and Supramolecular Chemistry of Guizhou Province, Institute of Applied Chemistry, Guizhou University, Guiyang, 550025, China.

^b Public Course Teaching Department, Qiannan Medical College for Nationalities, Duyun, 558000, China

^c Department of Chemistry, University of Hull, Hull HU6 7RX, U.K.

E-mail: gyhxxiaoxin@163.com or xxiao@gzu.edu.cn (Xin Xiao), mengtiehong19850@163.com (Tie-Hong Meng), C.Redshaw@hull.ac.uk (Carl Redshaw)

Contents

General experimental

Figure S1. Absorbance intensity of UV/vis spectra *versus* pH at 288 nm for LVFX (2×10^{-5} mol/L) and LVFX@Q[6] (LVFX: Q[6] = 1:1, 2×10^{-5} mol/L) complex.

Figure S2. ¹H NMR spectra of (i) Q[6]; (ii) in the presence of 1.0 equiv. of LVFX; (iii) LVFX.

Figure S3. ¹H NMR spectra of (i) LVFX@Q[6]; (ii) Q[6]-CDs; (iii) *N,N'*-DLH @Q[6].

Figure S4. (a) UV-vis absorption; (b) fluorescence spectra; (c) of LVFX (2×10^{-5} mol/L in aqueous solution, pH=7) in the presence of increased concentrations of Q[6], respectively ($\lambda_{\text{ex}}=288$ nm); (b, d), binding constant of Q[6] with LVFX guest. Insert (b) Job's plot of Q[6] with LVFX guest.

Figure S5. (i) ¹H NMR spectra of Q[6]; (ii) ¹H NMR spectra of Q[6]-CDs; (iii) ¹H NMR spectra of LVFX in D₂O at 25 °C, (where LVFX was used directly from

commercial sample, pristine Q[6] were obtained by dissolving their pure samples in DI water in Teflon autoclave and heated at 180 °C for 12 h).

Figure S6. FT-IR spectra of the LVFX, Q[6]-CDs, and Q[6].

Table S1. Assignments of the Bands of the Infrared Absorption Spectra for Q[6]-LVFX.

Table S2. Crystal data and structure refinement for N,N' -DLH@Q[6]·[CdCl₄]₂(H₃O)·9H₂O.

Figure S7. Scanning electron microscopy analysis of the Q[6]-CDs.

Figure S8. XRD pattern of the Q[6]-CDs.

Figure S9. XPS spectra of the Q[6]-CDs

Figure S10. Fluorescence decay time of the Q[6]-CDs

Figure S11. Quantum yields of the Q[6]-CDs at 430 nm in water

Figure S12. ¹H NMR spectrum of N,N' -DLH@Q[6]·[CdCl₄]₂(H₃O)·9H₂O

Figure S13. Asymmetric unit of N,N' -DLH@Q[6]·[CdCl₄]₂(H₃O)·9H₂O with atoms drawn as 30 % probability ellipsoids. Minor disorder is not shown.

Figure S14. The guest molecule with atoms drawn as 30 % probability ellipsoids. Minor disorder is not shown.

Figure S15. UV-vis absorption spectra obtained for Q[6]-CDs (20 µg/mL in neutral water) upon increasing the concentration of *L*-Trp in water.

Figure S16. Fluorescence spectra of probe-*L*-Trp and probe-*L*-Trp with other 19 amino acids.

Figure S17. ¹H NMR spectra of (i) Q[6]; (ii) in the presence of 1.0 equiv. of *L*-Trp; (iii) *L*-Trp.

Figure S18. ¹H NMR spectra of (i) Q[6]-CDs; (ii) in the presence of 1.0 equiv. of *L*-Trp; (iii) *L*-Trp.

Figure S19. ¹H NMR spectra of (i) *L*-Trp; (ii) in the presence of 1.0 equiv. of LVFX; (iii) LVFX.

Figure S20. UV-vis absorption spectra obtained for the Q[6]-CDs (20 µg/mL in neutral water) upon increasing the concentration of CAP in water.

Figure S21. ¹H NMR spectra of (i) Q[6]; (ii) in the presence of 0.5 equiv. of CAP; (iii)

in the presence of 1.0 equiv. of CAP; (iv) CAP.

Figure S22. ^1H NMR spectra of (i) Q[6]-CDs; (ii) in the presence of 1.0 equiv. of CAP; (iii) CAP.

Figure S23. ^1H NMR spectra of (i) CAP; (ii) in the presence of 1.0 equiv. of LVFX; (iii) LVFX.

References

Materials

Levofloxacin, tryptophan and capecitabine were purchased from Aladdin (Shanghai, China). Q[6] was prepared in the laboratory. All reagents were direct used without any further purification. Deionized (DI) water was used throughout the whole process.

Characterization

¹H NMR spectra were measured on JNM-ECZ400 MHz nuclear magnetic resonance (NMR) spectrometer. UV-vis spectra were recorded on an Agilent-8453 spectrophotometer. Fluorescence spectra measurements were performed on a Varian Cary Eclipse fluorescence spectrophotometer equipped with a xenon discharge lamp. Fourier transform infrared (FTIR) spectra recorded on a Bruker Vertex with KBr pellets.

The reactants of levofloxacin (LVFX) (20 mg, 0.0100 mmol) and cucurbit[6]uril (25 mg, 0.005 mmol) and CdCl₂ were dissolved in HCl (3 mol/L). The system was then heated at high temperature and cooled to room temperature. As LVFX is oxidized and degraded at high temperature to generate *N,N'*-DLH, the piperazine ring of LVFX is decomposed into an ethylenediamine group. And were then left to dry naturally in the open air. After standing for two days at room temperature, green block crystals of *N,N'*-DLH@Q[6] were collected by filtration, and then dried in air (yield: 50%, based on Q[6]). Anal. Calcd for C₅₂H₆₉Cd₂Cl₈FN₂₇O₂₃ (2023.73).

A suitable single crystal (0.18×0.14×0.13 mm³) was coated with paraffin oil and mounted on a Bruker D8 Advance X-ray diffractometer equipped with a graphite-monochromated Mo K α radiation source ($\lambda = 0.71073 \text{ \AA}$, $\mu = 0.828 \text{ mm}^{-1}$) operating in the ω -scan mode and fitted with a nitrogen cold stream (273.15 K). Data were corrected for Lorentz and polarization effects using (SAINT), and semiempirical adsorption corrections based on equivalent reflections were also applied using (SADABS). The structure was solved by dual space methods in SHELXT and the structure refined using SHELXL-2018 [1, 2] implemented within Olex2 [3].

All nonhydrogen atoms were refined anisotropically. Carbon-bound hydrogen atoms were introduced at calculated positions and were treated as riding atoms with an isotropic displacement parameter equal to 1.2 times that of the parent atom. Analytical

expressions for neutral-atom scattering factors were employed and anomalous dispersion corrections were incorporated.

Crystal Data for C₅₂H₇₇Cd₂Cl₈FN₂₇O₂₆ (M = 2023.73 g/mol): monoclinic, space group P2₁/c (no. 14), a = 16.7131(14) Å, b = 24.1071(19) Å, c = 20.6944(18) Å, β = 112.057(3)°, V = 7727.6(11) Å³, Z = 4, T = 223 K, μ(MoKα) = 0.924 mm⁻¹, Dcalc = 1.732 g/cm³, 85311 reflections measured (3.176° ≤ 2θ ≤ 51.7°), 14935 unique (Rint = 0.0849, Rsigma = 0.0575) which were used in all calculations. The final R₁ was 0.0970 and wR₂ was 0.1428 (all data). CCDC 2161127 contains the supplementary crystallographic data for this paper. These data can be obtained free of charge from The Cambridge Crystallographic Data Centre via www.ccdc.cam.ac.uk/data_request/cif. [Table S2](#) shows the crystal data and structure refinement for *N, N'*-DLH@Q[6].

¹H NMR spectra were recorded on a JEOL JMM-ECZ400s spectrometer at 25 °C. Using D₂O as a field frequency lock, the observed chemical shift is reported in parts per million (ppm) relative to the built-in tetramethylsilane (TMS) standard (0.0 ppm).

The calculation technique used for the LOD was based on the standard derivation of 10 measurements without the guest molecule (σ) and the slope of the linear calibration curve (K) based on the formula LOD = 3σ/K. The standard deviation of 10 measurements without the guest molecule could be determined based on the following

relationship:
$$\sigma = \sqrt{\frac{1}{n-1} \sum_{i=1}^n (x_i - \bar{x})^2}$$
, where n is the number of measurements (n=11).

Stock solutions of Q[6]-CDs (30 μg/mL) and amino acids (0.20 mol/L) were prepared in double-distilled water. amino acids including *L*-Ser, *L*-Aal, *L*-Phe, *L*-Asn, *L*-Leu, *L*-Thr, *L*-Pro, *L*-Lys, *L*-Arg, *L*-Tyr, *L*-Cys, *L*-Gly, *L*-Ala, *L*-Iso, *L*-Gln, *L*-L-Asp, *L*-Met, *L*-Glu, *L*-Trp and *L*-His. Working solutions were prepared by diluting stock solutions to the required concentrations.

Aqueous solutions of Q[6]-CDs (20 μg/mL) were prepared by diluting the stock solutions. The excitation and maximum emission wavelengths (λ_{ex}/λ_{em}) were 245 nm and 430 nm for the Q[6]-CDs.

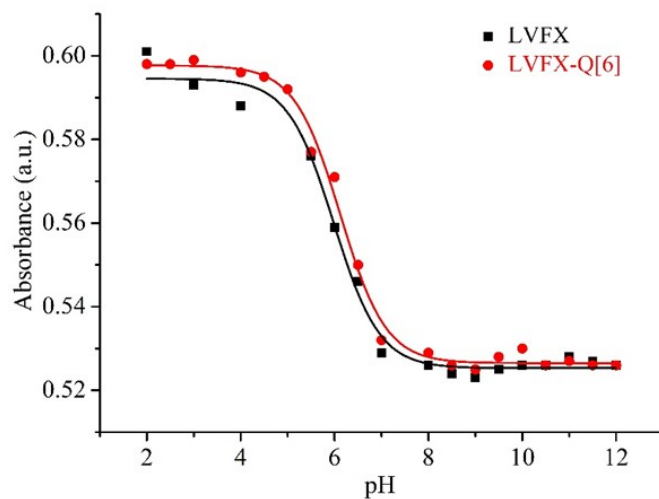


Figure S1. Absorbance intensity of UV/vis spectra *versus* pH at 288 nm for LVFX (2×10^{-5} mol/L) and LVFX@Q[6] (LVFX: Q[6] = 1:1, 2×10^{-5} mol/L) complex.

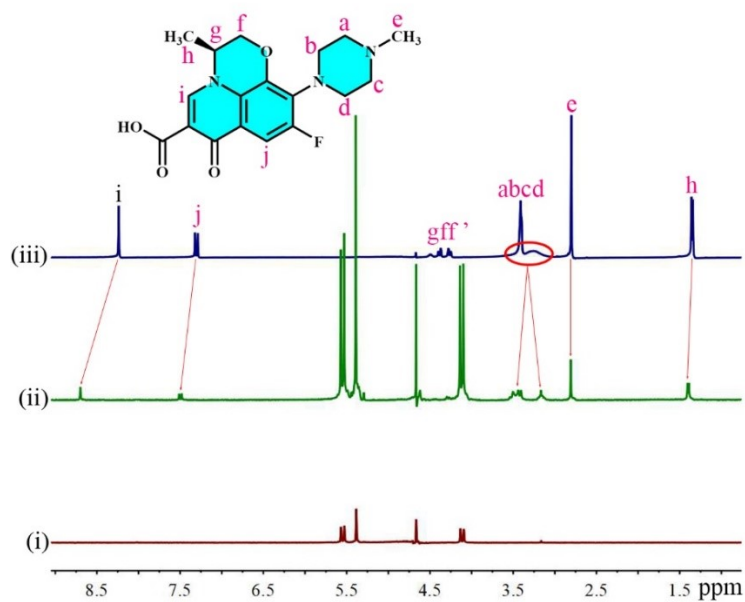


Figure S2. ^1H NMR spectra of (i) Q[6]; (ii) in the presence of 1.0 equiv. of LVFX; (iii) LVFX.

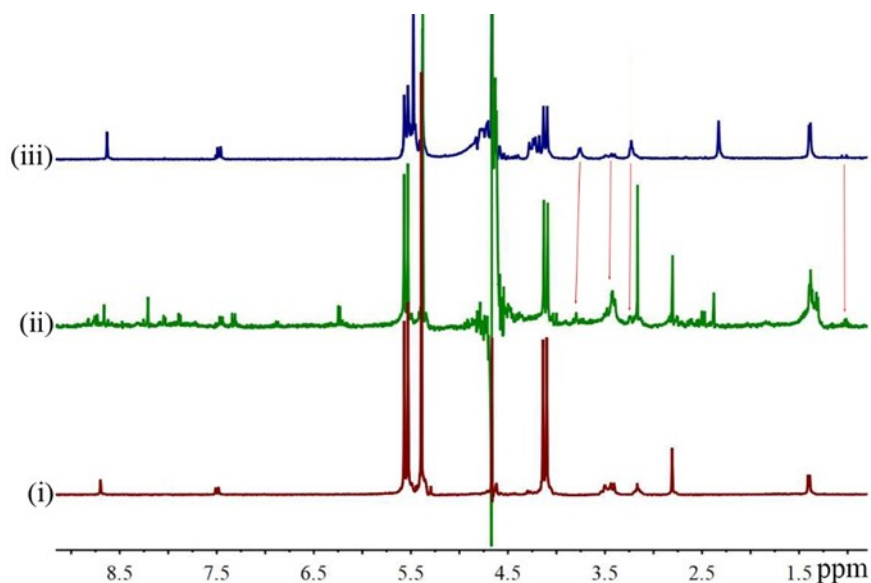


Figure S3. ^1H NMR spectra of (i) LVFX@Q[6]; (ii) Q[6]-CDs; (iii) N,N' -DLH@Q[6].

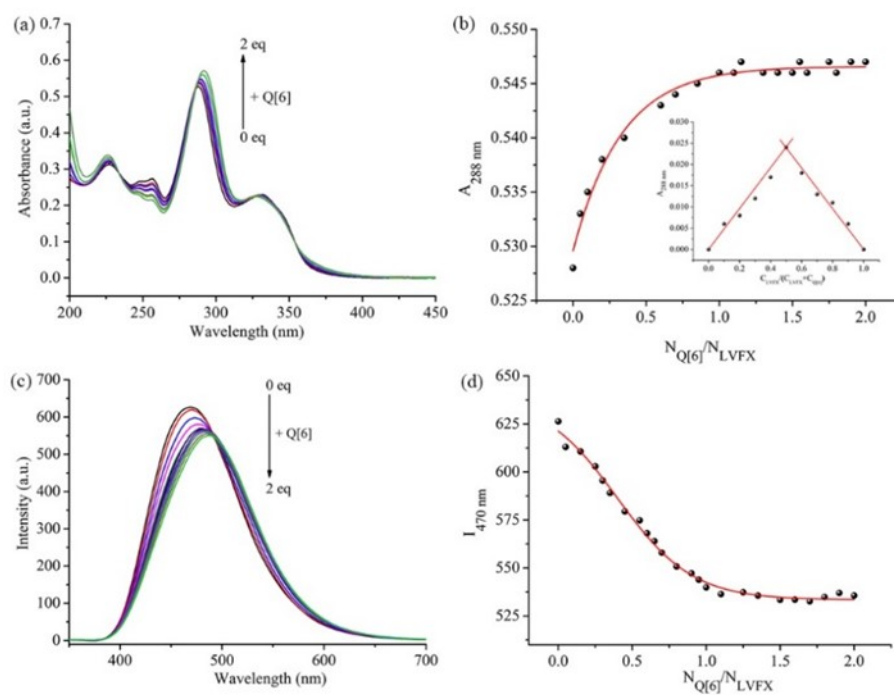


Figure S4. (a) UV-vis absorption; (b) fluorescence spectra; (c) of LVFX (2×10^{-5} mol/L in aqueous solution, pH=7) in the presence of increased concentrations of Q[6], respectively ($\lambda_{\text{ex}}=288$ nm); (b, d), binding constant of Q[6] with LVFX guest. Insert (b) Job's plot of Q[6] with LVFX guest.

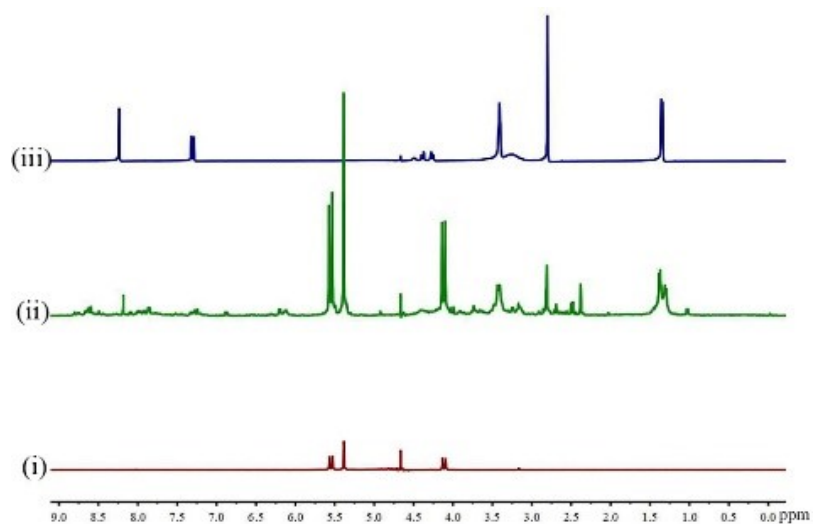


Figure S5. (i) ^1H NMR spectra of Q[6]; (ii) ^1H NMR spectra of Q[6]-CDs; (iii) ^1H NMR spectra of LVFX in D_2O at 25 °C, (where LVFX was used directly from commercial sample, pristine Q[6] were obtained by dissolving their pure samples in DI water in Teflon autoclave and heated at 180 °C for 12 h).

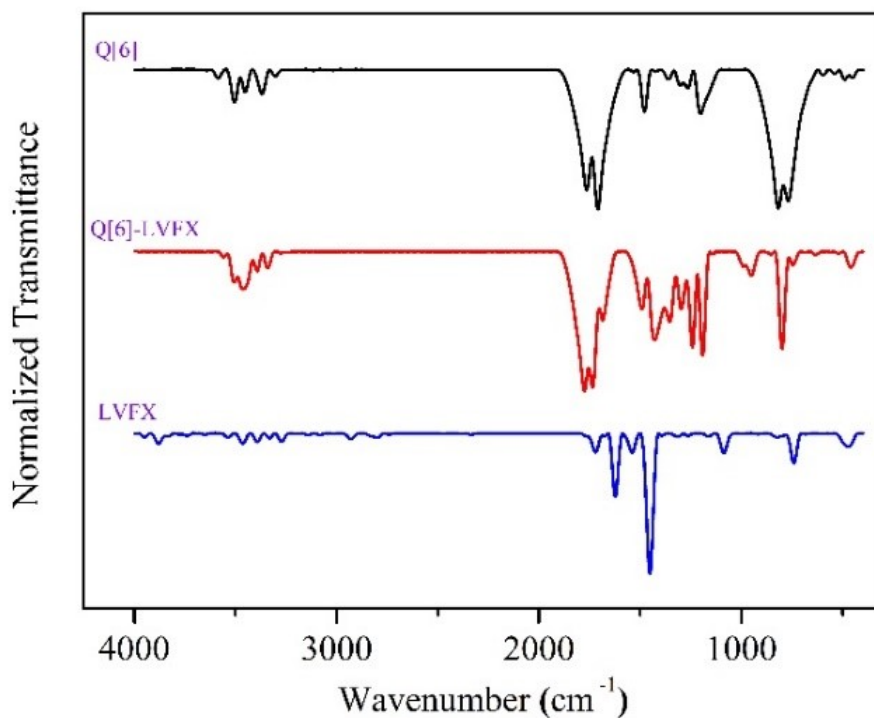


Figure S6. FT-IR spectra of the LVFX, Q[6]-CDs, and Q[6].

Table S1. Assignments of the Bands of the Infrared Absorption Spectra
for Q[6]-LVFX.

Observed IR (cm ⁻¹)	Attributions
3507	$\nu(\text{O-H})$
3464	$\nu(\text{O-H})$
3341	$\nu(\text{C-H})$
1774	$\nu(\text{C=O})$
1734	$\nu(\text{C=O})_{\text{carb}}$
1684	$\nu_{\text{s}}(\text{C=O})$
1490	$\delta_{\text{s}}(\text{C-H})$
1428	$\nu(\text{CH}_2)$ $\nu(\text{CH}_3)$, $\nu(\text{O-H})$
1353	$\beta(\text{CH}_2) + \omega(\text{CH}_2)$
1296	$\nu_{\text{s}}(\text{C-N})$
1241	$\nu_{\text{s}}(\text{C-N})$
1191	$\nu(\text{C=O-C-OH})$, $\nu(\text{C-H})$, $\nu(\text{all nucleus})$
950	$\beta(\text{C-H})$
852	$\gamma(\text{C-C-H})$
798	$\gamma_{\text{s}}(\text{C-C-H})$
745	$\nu(\text{piperazine nucleus})$, $\nu(\text{CH}_2)$, $\nu(\text{C-H})$ $\nu(\text{C-N})$
458	$\delta(\text{C-C-N})$

Table S2. Crystal data and structure refinement for *N,N'*-

Identification code	CCDC 2161127
Empirical formula	C ₅₂ H ₇₇ Cd ₂ Cl ₈ FN ₂₇ O ₂₆
Formula weight	2023.73
Temperature/K	273
Crystal system	monoclinic
Space group	P2 ₁ /c
a/Å	16.7131(14)
b/Å	24.1071(19)
c/Å	20.6944(18)
α/°	90
β/°	112.057(3)
γ/°	90
Volume/Å ³	7727.6(11)
Z	4
ρ _{calc} /cm ³	1.732
μ/mm ⁻¹	0.924
F(000)	4072.0
Crystal size/mm ³	0.22 × 0.21 × 0.21
Radiation	MoKα (λ = 0.71073)
2θ range for data collection/°	3.176 to 51.7
Index ranges	-20 ≤ h ≤ 20, -29 ≤ k ≤ 27, -25 ≤ l ≤ 25
Reflections collected	85311
Independent reflections	14935 [R _{int} = 0.0849, R _{sigma} = 0.0575]
Data/restraints/parameters	14935/0/1077
Goodness-of-fit on F ²	1.099
Final R indexes [I >= 2σ (I)]	R ₁ = 0.0614, wR ₂ = 0.1277
Final R indexes [all data]	R ₁ = 0.0970, wR ₂ = 0.1428
Largest diff. peak/hole / e Å ⁻³	0.83/-0.66

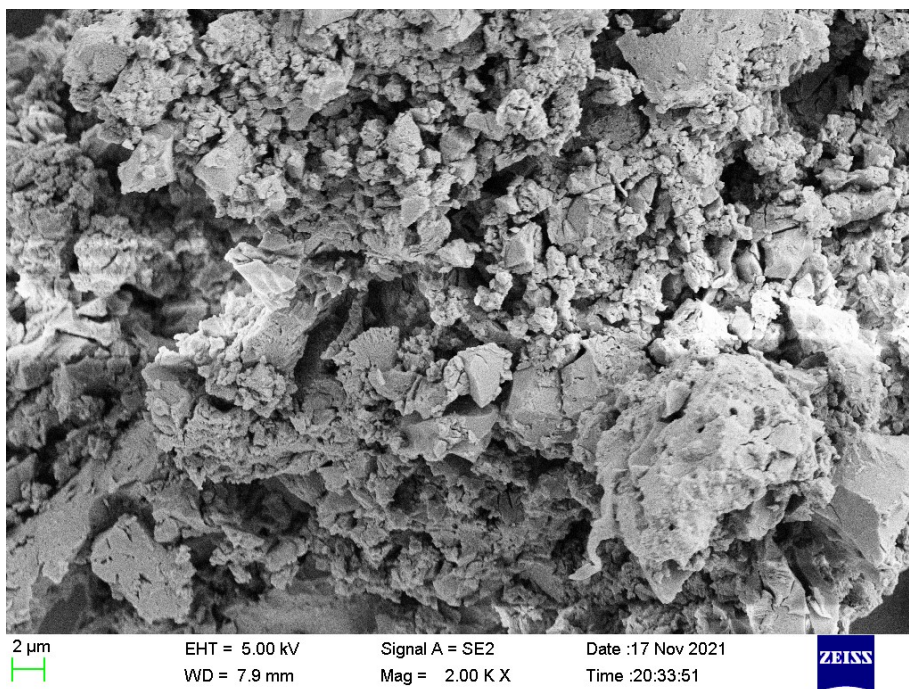


Figure S7. Scanning electron microscopy analysis of the Q[6]-CDs.

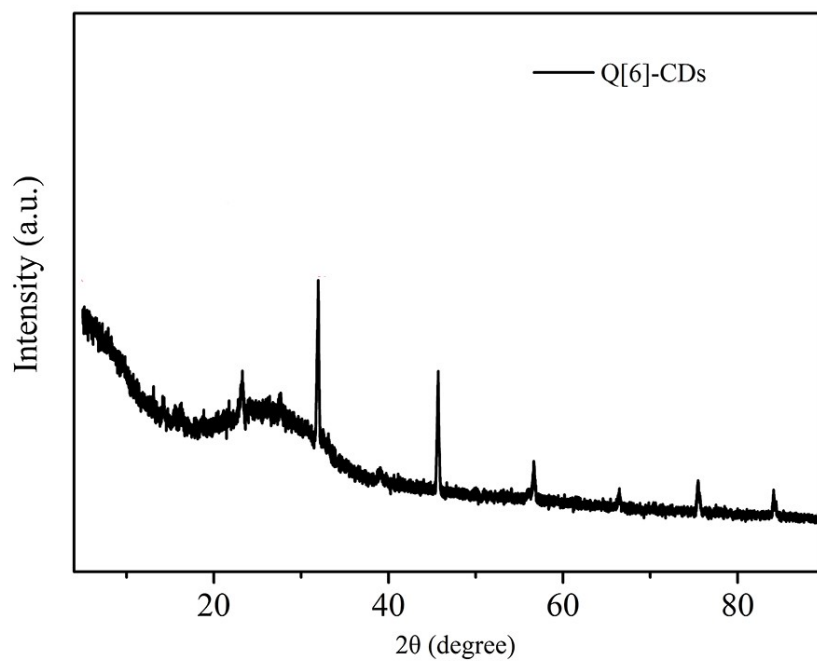


Figure S8. XRD pattern of the Q[6]-CDs.

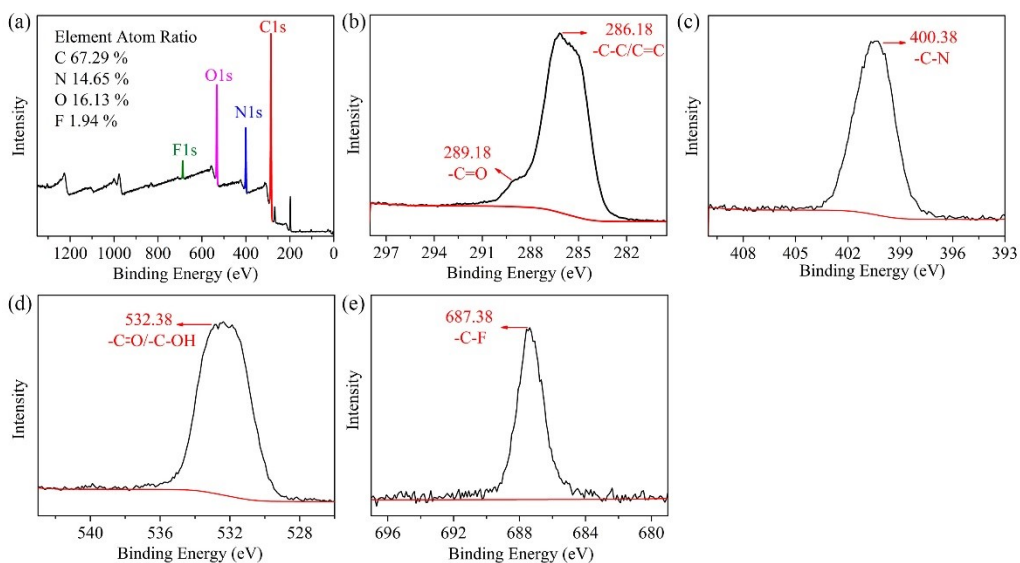


Figure S9. (a) XPS spectra of the Q[6]-CDs; (b, c, d and e) high resolution spectra of C1s, N1s, O1s and F1s, respectively.

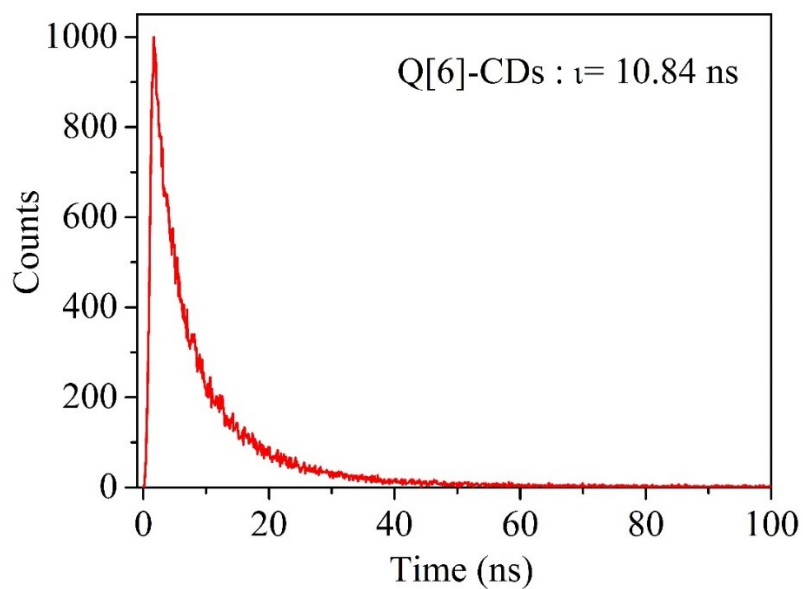


Figure S10. Fluorescence decay time of the Q[6]-CDs.

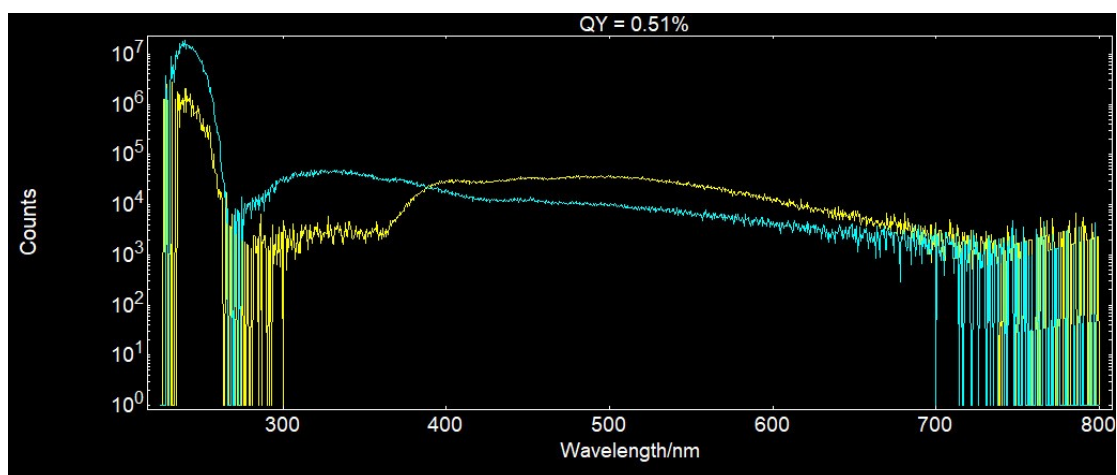


Figure S11. Quantum yields of the Q[6]-CDs at 430 nm in water.

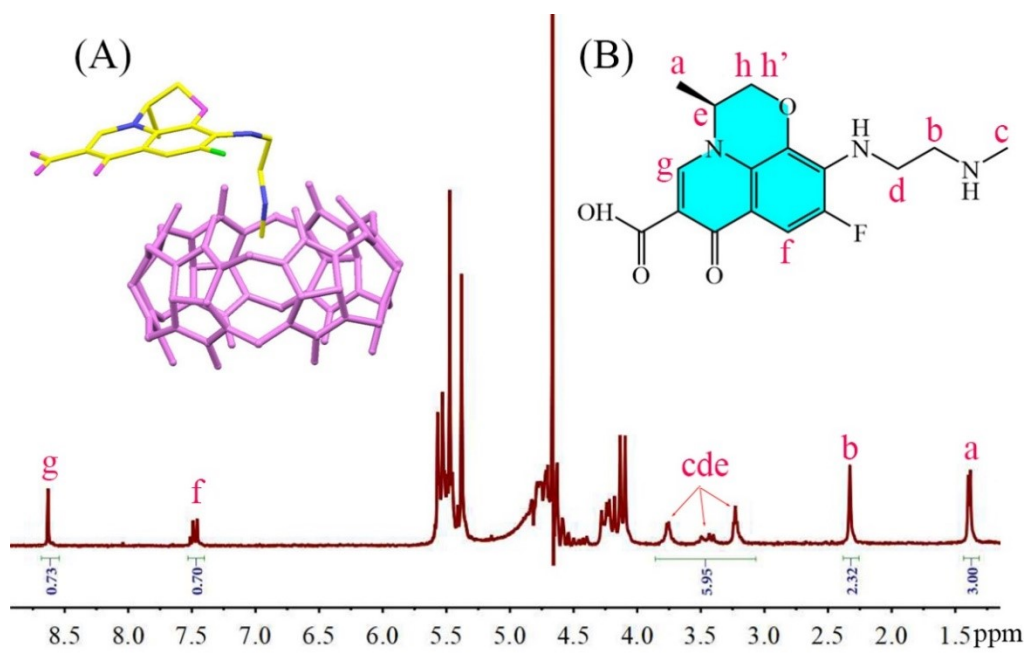


Figure S12. ^1H NMR spectrum of N,N' -DLH@Q[6].[CdCl₄]₂(H₃O).9H₂O.

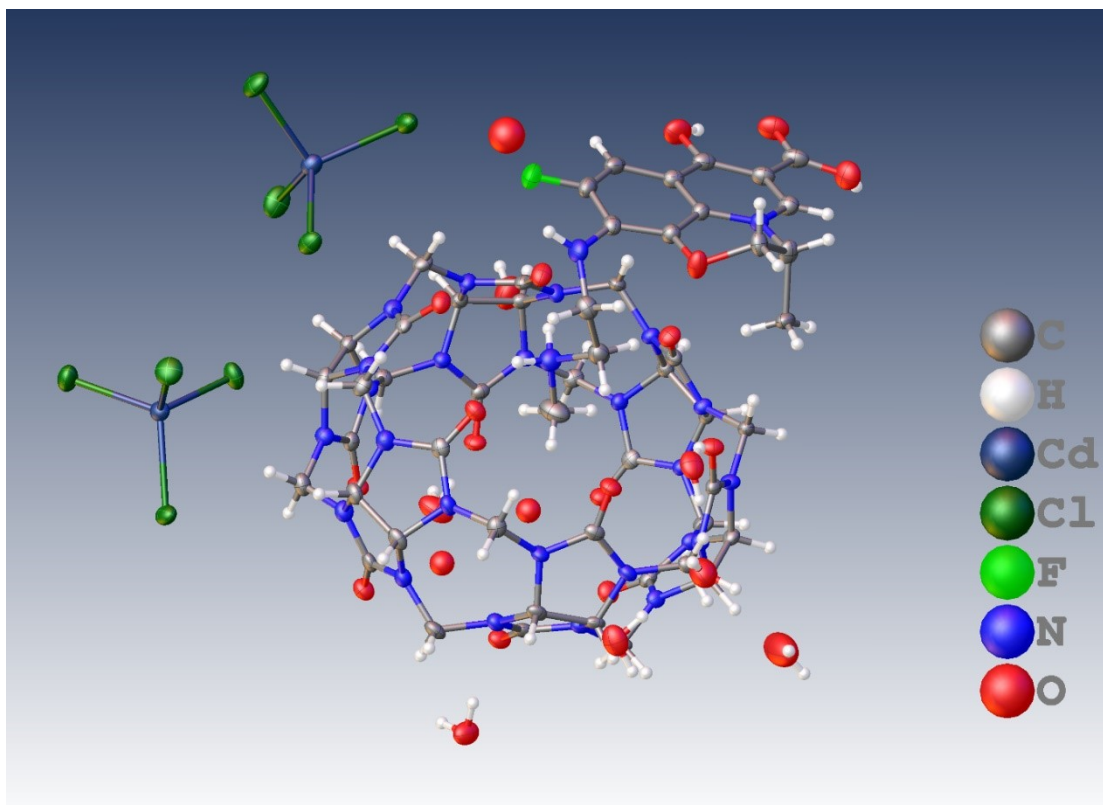


Figure S13. Asymmetric unit of N,N' -DLH@Q[6].[CdCl₄]₂(H₃O).9H₂O with atoms drawn as 30 % probability ellipsoids. Minor disorder is not shown.

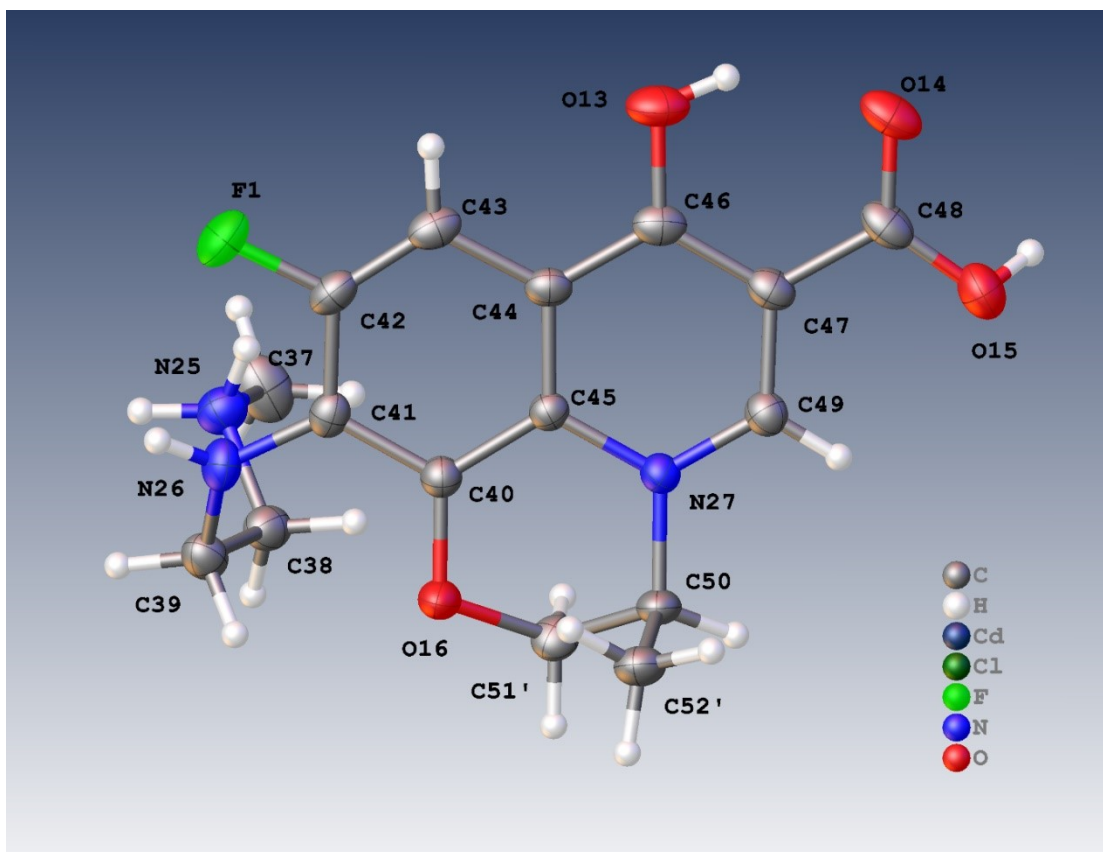


Figure S14. The guest molecule with atoms drawn as 30 % probability ellipsoids. Minor disorder is not shown.

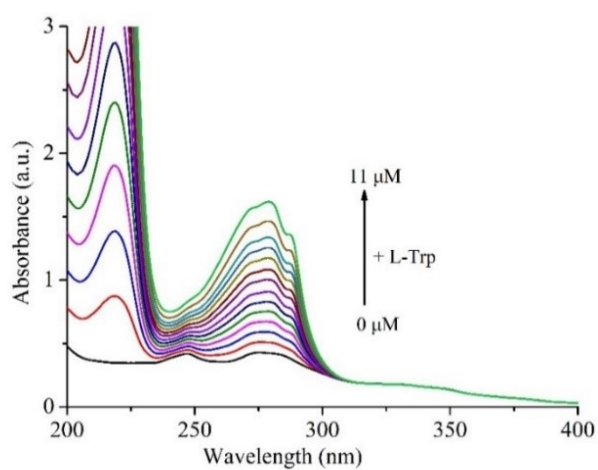


Figure S15. UV-vis absorption spectra obtained for the Q[6]-CDs (20 µg/mL in neutral water) upon increasing the concentration of *L*-Trp in water.

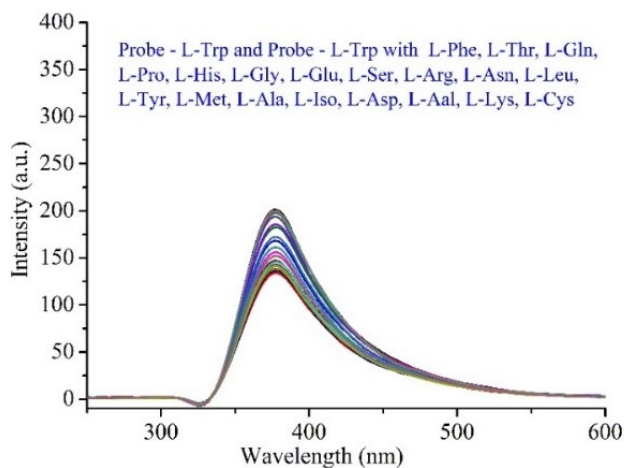


Figure S16. Fluorescence spectra of probe-*L*-Trp and probe-*L*-Trp with other 19 amino acids.

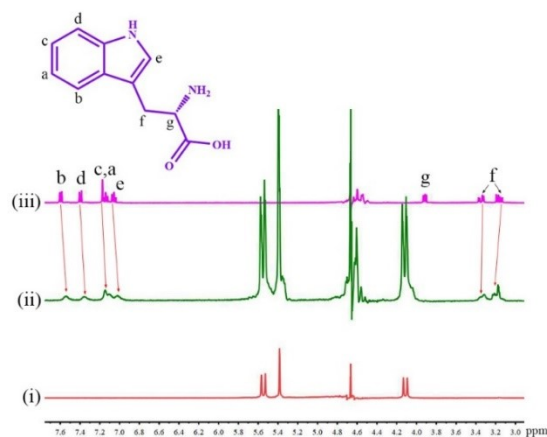


Figure S17. ^1H NMR spectra of (i) Q[6]; (ii) in the presence of 1.0 equiv. of *L*-Trp; (iii) *L*-Trp.

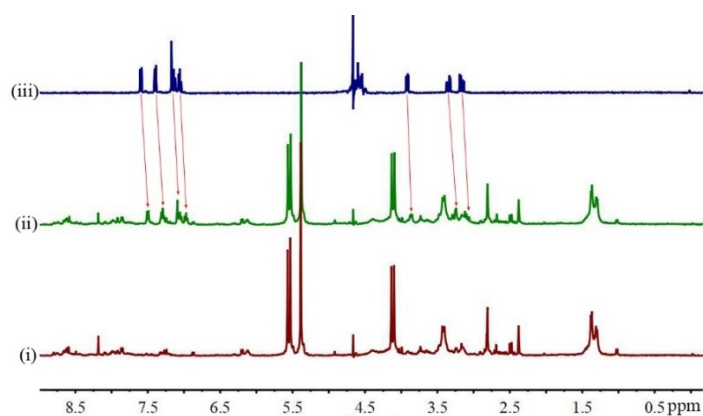


Figure S18. ^1H NMR spectra of (i) Q[6]-CDs; (ii) in the presence of 1.0 equiv. of *L*-Trp; (iii) *L*-Trp.

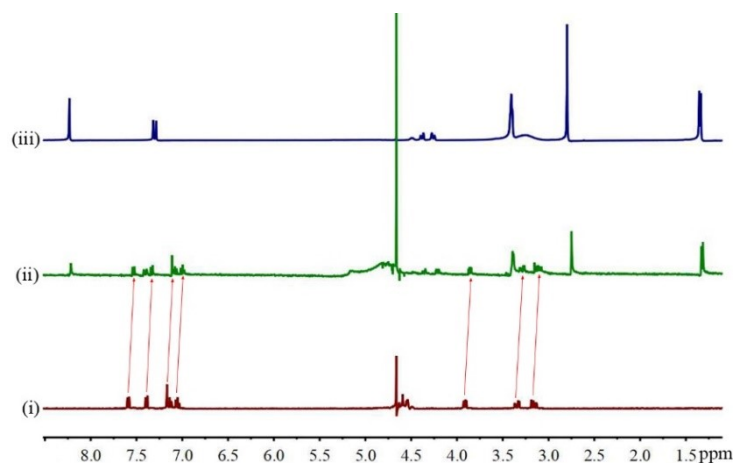


Figure S19. ^1H NMR spectra of (i) *L*-Trp; (ii) in the presence of 1.0 equiv. of LVFX; (iii) LVFX.

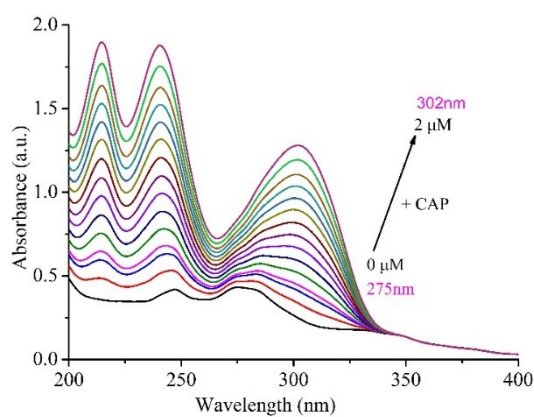


Figure S20. UV-vis absorption spectra obtained for Q[6]-CDs (20 $\mu\text{g}/\text{mL}$ in neutral water) upon increasing the concentration of CAP in water.

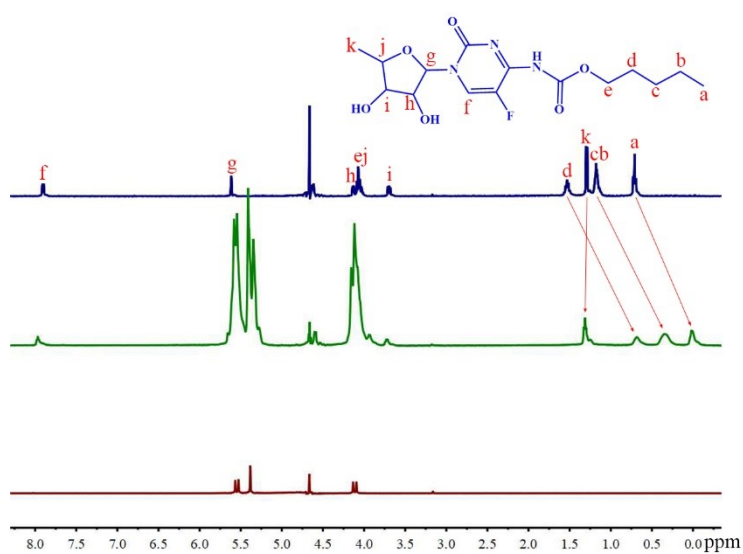


Figure S21. ^1H NMR spectra of (i) Q[6]; (ii) in the presence of 0.5 equiv. of CAP; (iii) in the presence of 1.0 equiv. of CAP; (iv) CAP.

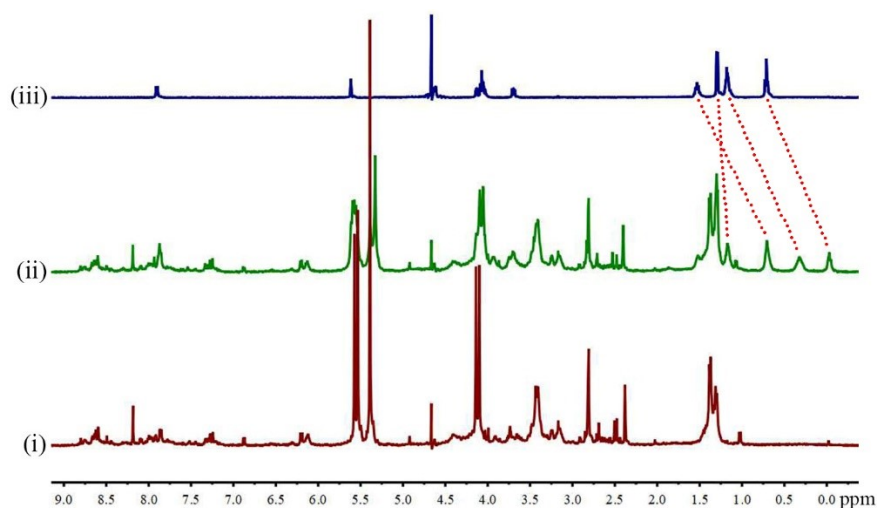


Figure S22. ^1H NMR spectra of (i) Q[6]-CDs; (ii) in the presence of 1.0 equiv. of CAP; (iii) CAP.

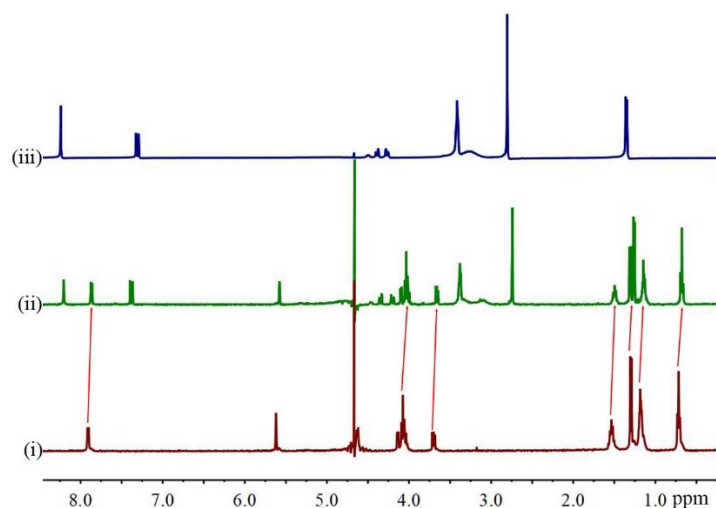


Figure S23. ^1H NMR spectra of (i) CAP; (ii) in the presence of 1.0 equiv. of LVFX; (iii) LVFX.

References

- [1] G. M. Sheldrick. *Acta Crystallogr. Sect. A*, **2008**, *64*, 112–122.
- [2] G. M. Sheldrick, Crystal structure refinement with SHELXL, *Acta Cryst.* **2015**, *C71*, 3-8.
- [3] O. V. Dolomanov, L. J. Bourhis, R. J. Gildea, J. A. K. Howard, & H. Puschmann, OLEX2: a complete structure solution, refinement and analysis program, *J. Appl. Cryst.* **2009**, *42*, 339-341.